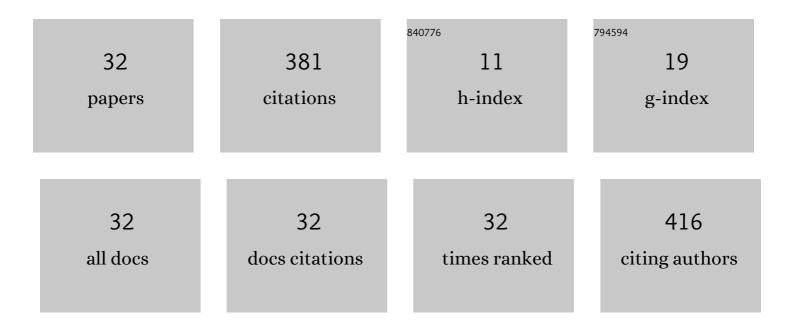
Thomas Mehner

List of Publications by Year in descending order

Source: https://exaly.com/author-pdf/7925106/publications.pdf Version: 2024-02-01



#	Article	IF	CITATIONS
1	Microstructure and Wear Resistance of AlCoCrFeNiTi High-Entropy Alloy Coatings Produced by HVOF. Coatings, 2017, 7, 144.	2.6	70
2	Influence of Titanium on Microstructure, Phase Formation and Wear Behaviour of AlCoCrFeNiTix High-Entropy Alloy. Entropy, 2018, 20, 505.	2.2	68
3	Wear-resistant coatings on aluminium produced by plasma anodising—A correlation of wear properties, microstructure, phase composition and distribution. Surface and Coatings Technology, 2014, 240, 96-102.	4.8	31
4	The Phase Composition and Microstructure of AlxCoCrFeNiTi Alloys for the Development of High-Entropy Alloy Systems. Metals, 2017, 7, 162.	2.3	29
5	Effect of additive and current mode on surface morphology of palladium films from a non-aqueous deep eutectic solution (DES). Journal of Applied Electrochemistry, 2013, 43, 1207-1216.	2.9	25
6	Effect of Strain Localization on Pitting Corrosion of an AlMgSi0.5 Alloy. Metals, 2015, 5, 172-191.	2.3	25
7	Electrodeposition of Pd alloys from choline chloride/urea deep eutectic solvents. Journal of Alloys and Compounds, 2021, 855, 157462.	5.5	16
8	Hydrogen embrittlement of a quenching and partitioning steel during corrosion and zinc electroplating. Materials Science & Engineering A: Structural Materials: Properties, Microstructure and Processing, 2019, 744, 247-254.	5.6	15
9	Microstructure and Corrosion Properties of AlCrFeCoNi High-Entropy Alloy Coatings Prepared by HVAF and HVOF. Journal of Thermal Spray Technology, 2022, 31, 247-255.	3.1	15
10	Measurement system based on the Seebeck effect for the determination of temperature and tool wear during turning of aluminum alloys. Procedia CIRP, 2020, 93, 1435-1441.	1.9	13
11	Residual-stress evolution of cold-rolled DC04 steel sheets for different initial stress states. Finite Elements in Analysis and Design, 2018, 144, 76-83.	3.2	11
12	Strain-rate sensitive ductility in a low-alloy carbon steel after quenching and partitioning treatment. Scientific Reports, 2019, 9, 17023.	3.3	9
13	Characterisation Method of the Passivation Mechanisms during the pre-discharge Stage of Plasma Electrolytic Oxidation Indicating the Mode of Action of Fluorides in PEO of Magnesium. Coatings, 2020, 10, 965.	2.6	9
14	Surface properties in turning of aluminum alloys applying different cooling strategies. Procedia CIRP, 2022, 108, 246-251.	1.9	7
15	Pulse plating of Pd–Ag alloy films from deep eutectic solvents. Surface Engineering, 2019, 35, 1081-1087.	2.2	6
16	Method for process monitoring of surface layer changes in turning of aluminium alloys using tools with a flank face chamfer. Procedia CIRP, 2020, 87, 432-437.	1.9	5
17	Comparative Investigation of Hydrogen Embrittlement of Palladium Deposits from Ionic Liquid and Aqueous Electrolyte. Advanced Engineering Materials, 2015, 17, 167-171.	3.5	4
18	Phosphorus Distribution in Electrodeposited Ni-P-Diamond Composites Influencing Structure and Mechanical Properties. Advanced Materials Research, 2013, 829, 105-109.	0.3	3

THOMAS MEHNER

#	Article	IF	CITATIONS
19	Irregular Electrodeposition of Cu-Sn Alloy Coatings in [EMIM]Cl Outside the Glove Box with Large Layer Thickness. Coatings, 2021, 11, 310.	2.6	3
20	Stabilization of the Computation of Stability Constants and Species Distributions from Titration Curves. Computation, 2021, 9, 55.	2.0	3
21	Analytical Model to Calculate the Grain Size of Bulk Material Based on Its Electrical Resistance. Metals, 2021, 11, 21.	2.3	3
22	Separation of Corrosion-affecting Parameters of Formed Products – A New Strategy Using X-ray Diffraction and Corrosion Tests Under in-situ Tensile Load. Materials Today: Proceedings, 2015, 2, S141-S148.	1.8	2
23	Influence of SiC particle volume fraction and texture on the surface properties in milling of AMCs with MCD-tipped tools. Procedia CIRP, 2019, 85, 90-95.	1.9	2
24	On a Robust and Efficient Numerical Scheme for the Simulation of Stationary 3-Component Systems with Non-Negative Species-Concentration with an Application to the Cu Deposition from a Cu-(β-alanine)-Electrolyte. Algorithms, 2021, 14, 113.	2.1	2
25	Structural Characterization and Wear Investigations of Palladium Layers Electrochemically Deposited Using Ionic Liquids. Advanced Engineering Materials, 2013, 15, 1115-1121.	3.5	1
26	Simultaneous Electrodeposition of Silver and Tungsten from [EMIm]Cl:AlCl3 Ionic Liquids outside the Glove Box. Coatings, 2020, 10, 553.	2.6	1
27	Mechanical test procedures for the evaluation of hydrogen-assisted damage in high-strength steel. Materialpruefung/Materials Testing, 2019, 61, 1061-1071.	2.2	1
28	Metrological characterization of the thermomechanical influence of the cross-section of the undeformed chip on the surface properties in turning of the aluminum alloy EN AW-2017. TM Technisches Messen, 2020, 87, 777-786.	0.7	1
29	Mathematical Modeling of the Limiting Current Density from Diffusion-Reaction Systems. Axioms, 2022, 11, 53.	1.9	1
30	Detection and Prediction of Corrosion-Affecting Parameters in Cold Flat Rolling Processes. Procedia Engineering, 2017, 184, 22-29.	1.2	0
31	Archaeometric case studies on decorations of preâ€Columbian pottery using Xâ€ray spectroscopy maps and profiles. Materialwissenschaft Und Werkstofftechnik, 2017, 48, 485-494.	0.9	Ο
32	Metal Foils for Bipolar Plates—Correlation of Initial Grain Size and Forming Behavior of 316L. Minerals, Metals and Materials Series, 2021, , 1743-1756.	0.4	0